Research Square

Preprints are preliminary reports that have not undergone peer review.
They should not be considered conclusive, used to inform clinical practice,
or referenced by the media as validated information.

Development and validation of hyperlipidemia-related genes for prognosis prediction in colorectal cancer

Kunpeng Bu
Tumor Hospital of Guangxi Medical University
Peigeng He
Tumor Hospital of Guangxi Medical University
Haiyan Huang
huanghaiyan005@163.com

Tumor Hospital of Guangxi Medical University
Yue Wu
Tumor Hospital of Guangxi Medical University
Jinliang Kong
First Affiliated Hospital of GuangXi Medical University
Tianwen Huang
Tumor Hospital of Guangxi Medical University

Article

Keywords: Colorectal cancer, Hyperlipidemia-related genes, Biomarkers, Immune infiltration, Drug prediction

Posted Date: April 12th, 2026

DOI: https://doi.org/10.21203/rs.3.rs-8039900/v1

License: This work is licensed under a Creative Commons Attribution 4.0 International License.
Read Full License

Additional Declarations: No competing interests reported.

Abstract

Background: Colorectal cancer (CRC) often presents with high mortality and a poor prognosis. Numerous studies have demonstrated the association between hyperlipidemia and CRC metastasis. This study aimed to characterize hyperlipidemia-related genes (HRGs) and thereby lay a theoretical foundation for the early diagnosis and treatment of CRC.

Methods: We derived differentially expressed HRGs (DE-HRGs) by intersecting differentially expressed genes, Weighted Gene Co-expression Network Analysis (WGCNA) key module genes, and predefined HRGs from the TCGA-CRC and GSE39582 datasets. Protein-Protein Interaction (PPI)s were employed, followed by the application of machine learning for subsequent identification of biomarkers. Following validation of biomarker expression in the TCGA-CRC and GSE39582 datasets, their diagnostic value was assessed by receiver operating characteristic (ROC) analysis. Further investigations encompassed Kaplan-Meier survival analysis, nomogram development, immune infiltration profiling, regulatory network mapping, and drug prediction, culminating in quantitative reverse transcription polymerase chain reaction (qRT-PCR) confirmation.

Results: A total of 44 DE-HRGs were identified. GCG, SST, SLC30A10, and SLC22A5 were identified as biomarkers associated with hyperlipidemia and affecting the progression of CRC, which could effectively diagnose CRC patients in both datasets. A significant difference in GCG expression was found between the risk groups via survival analysis. Meanwhile, the nomogram constructed based on biomarkers exhibited an excellent prediction effect for CRC patients. Through immune infiltration analysis, it was found that activated CD8 T cells had a striking positive correlation with SST and a significant negative correlation with SLC22A5. The established regulatory network contained 4 mRNAs, 11 miRNAs, and 17 lncRNAs, and the regulatory relationships included

LINC01915-Hsa-miR-450b-5p-SLC30A10 and others. 16 therapeutic drugs were predicted, such as Naltrexone, Streptozocin, and Carnitine, et al. Importantly, the qRT-PCR results showed that the biomarkers had down-regulated expression in the CRC group, and the direction of this expression trend was consistent with that of the datasets.

Conclusion: The identification of GCG, SST, SLC30A10, and SLC22A5 as hyperlipidemia-related biomarkers in CRC contributes a scientific basis for future research.

1. Introduction

Colorectal cancer (CRC) is the third most common aggressive malignancy and the second-leading cause of cancer-related deaths worldwide[1]. The pathogenesis of CRC is a complicated process involving mutations of various oncogenes and tumor suppressor genes that pinpoint multiple cellular events, such as endoplasmic reticulum stress[2], oxidative stress[3], epithelial-mesenchymal transition (EMT)[4], abnormal cell proliferation, and apoptosis[5]. Early-stage colorectal cancer often presents atypical symptoms, typically manifesting as changes in bowel habits (alternating diarrhea and constipation) and

abnormal stool characteristics (such as bloody stools or thinner stools). As the disease progresses, patients may develop characteristic symptoms including abdominal pain, abdominal masses, intestinal obstruction, anemia, and weight loss [6]. The development of colorectal cancer results from multiple interacting factors. Modifiable risk factors such as lifestyle and dietary habits are the primary focus of prevention, while non-modifiable factors like genetic predisposition and age require early intervention through regular screening[7]. The high rates of tumor recurrence and metastasis in CRC lead to unsatisfactory patient prognosis, despite considerable advances in treatment modalities[8,9]. CRC cases are expected to increase substantially to 66%, from 1.93 million in 2020 to 3.20 million in 2040[10]. Therefore, early identification of CRC features is crucial for early diagnosis and intervention of patients.

Recently, much evidence has shown that the prevalence of CRC is associated with diet and dietary fiber intake, thus highlighting the meaningful relationship between diet and CRC[8,9,11]. Clinically, many epidemiological reports suggest that a lifestyle leading to high lipid levels, such as a high-fat diet (HFD) status, stimulates the progression of CRC[12], and the use of statins can significantly reduce the mortality of those patients[13]. Notably, obesity caused by a high-fat lifestyle often results in abnormal adipose tissue metabolism, affecting the release of free fatty acids, enzymes, hormones, inflammatory cytokines, growth factors, and other factors[14]. These metabolites are considered significant risk indicators for the morbidity and mortality of CRC. Moreover, the adipocyte-cancer cell interactions cause changes in the morphology and function of adipose tissue, resulting in changes to paracrine and endocrine signals[15,16]. In contrast, metabolites released after physiological changes in adipose tissue can significantly promote CRC cells' proliferation, invasion, and metastasis[17]. Given the significant impact of hyperlipidemia on CRC prognosis, there is a need to explore its associated features and develop specific models for patient identification.

In this study, we obtained CRC-related datasets from the University of California Santa Cruz (UCSC) xena database and Gene Expression Omnibus (GEO) database, and hyperlipidemia-related genes (HRGs) from GeneCards, DisGeNET and DrugBANK databases. The identification of hyperlipidemia-related biomarkers in CRC via bioinformatics analyses offers potential targets for clinical diagnosis and prognosis, as well as a theoretical basis for further mechanistic investigation.

2. Materials and Methods

2.1 Data Extraction

The RNA-seq and clinical data of The Cancer Genome Atlas-colon adenocarcinoma (TCGA-COAD) and The Cancer Genome Atlas-rectum adenocarcinoma (TCGA-READ) were gained from the UCSC xena database (https://xenabrowser.net), which were combined to create The Cancer Genome Atlas-Colorectal cancer (TCGA-CRC). The training set consisted of 51 normal and 638 CRC tissue samples. The GSE39582 dataset, which included 19 normal and 443 CRC tissue samples, was retrieved as a validation set from the GEO database (https://www.ncbi.nlm.nih.gov/). In total, 2,314 HRGs were

identified using the results of GeneCards (www.genecards.org), DisGeNET (http://www.disgenet.org), and DrugBANK (www.drugbank.ca) databases.

2.2 Differential expression analysis

Identification of differentially expressed genes (DEGs) between CRC and control samples was performed using the DESeq2 package (version 3.50.3)[18], based on the threshold value as adjust $p \leq 0.05$ and $|\log_2 FoldChange(FC)| \geq 1$.

2.3 Weighted Gene Co-expression Network Analysis (WGCNA)

A co-expression network of CRC patients was established using the R package WGCNA (version 1.71) [19], which identified module genes correlated with CRC. Firstly, the sample clustering was deployed to recognize and eliminate outliers. A scale-free co-expression network was constructed by selecting an optimal soft threshold, following which the dynamic tree-cutting algorithm was applied to identify modules, each containing a minimum of 50 genes. Correlation analysis identified modules strongly associated with CRC, which were designated as key modules, and their constituent genes were defined as key module genes.

2.4 Identification of hub genes

The intersection of the HRGs, DEGs, and key module genes was identified using the ggVennDiagram package (version 1.2.2)[20]. These genes were defined as differentially expressed hyperlipidemia-related genes (DE-HRGs). Enrichment analysis was performed on HR-DEGs using the clusterProfiler package (version 4.6.2)[21], including GO and KEGG ($p < 0.05$). Furthermore, to investigate the interaction between HR-DEGs, a PPI network was constructed utilizing the STRING database (http://string.embl.de/). The top 30 intersection genes were calculated by MCC, MNC, EPC, DMNC, and Degree of cytoHubba plug-ins in Cytoscape. These genes were defined as hub genes.

2.5 Screening and validation of biomarkers

LASSO regression[22] combined with the Boruta algorithm screened characteristic genes, which were then intersected with hub genes using the UpSetR package (version 1.4.0)[23] to establish the diagnostic biomarkers. For evaluation of diagnostic ability, ROC curves were plotted via the pROC package (version 1.18.0)[24] applied to both datasets.

2.6 Kaplan-Meier (K-M) survival analysis

We first stratified the training set samples into high- and low-expression groups based on the median biomarker level, and then assessed survival differences using K-M analysis with the survival (version 3.2-13) and survminer (version 0.4.9) packages[25] On the other hand, clinical information was collected from the TCGA-CRC dataset, and a K-M survival analysis was conducted for various clinical characteristics of

CRC, such as age, gender, stage, T stage, N stage, and M stage. To compare the distribution differences of clinical features between groups with high and low biomarker expression, a Chi-square test was used.

2.7 Nomogram drawing of biomarkers

The rms package (version 6.3-0)[25] created the biomarkers nomogram in the training set. The calibration curve served to evaluate the accuracy of the nomogram.

2.8 Functional enrichment analysis of biomarkers

We first calculated and sorted the Pearson correlation coefficients between each biomarker and all genes in the training set. We then performed GSEA on KEGG pathways using the clusterProfiler package (version 4.6.2)[21]. Using the FDR method for multiple test correction resulted in p.adjust < 0.05, which were deemed significant enrichment outcomes.

2.9 Immune Infiltration Analysis

Using the GSVA package (version 1.42.0), ssGSEA was performed on CRC and normal groups to determine the infiltration scores of 28 immune cells[26]. The Wilcox test was utilized to compare the scores of the CRC and normal groups. Following visualization with the ggplot2 package (version 3.3.6) [27], using Spearman's method, we examined the correlation of key genes with differential immune cell infiltration.

2.10 Construction of molecular regulatory network

A molecular regulatory network was established to understand the regulatory mechanisms of biomarkers. We performed differential analysis of miRNAs and lncRNAs in normal versus CRC samples with the DESeq2 package (version 3.50.3)[18], applying thresholds of |log2FC| > 0.5 and p < 0.05 to identify DE-miRNAs and DE-lncRNAs. Then, the miRnet database was used to forecast miRNAs that bind to biomarkers. These predicted miRNAs were subsequently intersected with the DE-miRNAs to identify the key miRNAs. Prediction of lncRNAs via the starBase database, followed by their intersection with DE-lncRNAs, yielded the set of key lncRNAs. Finally, the miRNAs and biomarkers with regulatory relationships were extracted based on the final lncRNAs, and the network of biomarkers, miRNAs, and lncRNAs with regulatory relationships was carried out through Cytoscape software.

2.11 Drug prediction and molecular docking

The Drug-Gene Interaction database (DGIDB) (https://dgidb.org) was interrogated to identify potential drugs targeting the biomarkers and their interactions. The network was visualized using the Cytoscape software. A molecular docking approach was implemented to identify the drug with the highest binding affinity. Firstly, the Uniprot database (https://www.uniprot.org/) downloads the crystal structure corresponding to each biomarker. Next, AutoDock Vina was used to carry out molecular docking after

the small molecule drug's 3D structure was obtained from the PubChem database (https://pubchem.ncbi.nlm). Ultimately, the results were loaded into the PyMOL software to be seen.

2.12 Quantitative real-time polymerase chain reaction (qRT-PCR)

To validate the bioinformatics findings, qRT-PCR was performed on 10 paired clinical CRC and paracancerous tissues. Following extraction with TRIzol (Ambion), total RNA was reverse-transcribed into cDNA using the SureScript kit (Servicebio) as per the manufacturers' protocols. qPCR was then conducted with 2xUniversal Blue SYBR Green Master Mix (Servicebio). Gene expression was normalized to GAPDH and calculated via the $2^{-\Delta\Delta Ct}$ method, using primers listed in **Additional file 1**[28].

3. Results

3.1 DE-HRGs were associated with CRC

Using the criteria of |log2FC| ≥ 0.5 and adjusted p ≤ 0.05, the differential expression analysis yielded 5,102 DEGs between CRC and control groups. This set comprised 2,599 up-regulated and 2,503 down-regulated genes (**Fig. 1a-b**). Further, an outlier sample was eliminated (**Additional file 2**). Soft threshold 12 (R^2 = 0.85) was chosen to get a scale-free network as much as possible (**Fig. 1c**). After applying the dynamic tree cutting algorithm and merging similar modules, 13 co-expression modules were identified (**Fig. 1d**). Furthermore, MEpurple, as key module, was the highest positive association with CRC (correlation coefficient = -0.75, p < 0.05) (**Fig 1e**). After that, 310 key module genes were obtained. Finally, the intersection of 5,102 DEGs, 310 key module genes, and 2,314 HRGs was applied to obtain 44 DE-HRGs (**Fig. 1f**).

3.2 Functional enrichment analysis of 44 DE-HRGs

233 GO items and 3 KEGG pathways were associated with DE-HRGs. The GO items included 239 BP, 3 CC, and 28 MF. The GO analysis suggested that long-chain fatty acid transport, positive regulation of secretion, cellular lipid catabolic process, and fatty acid binding may be involved in hyperlipidemia. KEGG analysis showed that DE-HRGs were enriched in PPAR signaling pathways, bile secretion, fat digestion, and absorption. Based on the p-value ranking, the top 3 of each part of the GO terms (**Fig. 2a**) and KEGG pathways (**Fig. 2b**) were selected for displaying.

3.3 PPI analysis of 44 DE-HRGs

The PPI network of 44 DE-HRGs, built employing a 0.4 minimum interaction score, yielded 44 nodes and 241 edges (**Fig. 3a**). Twenty-eight hub genes were screened by five algorithms (**Fig. 3b**), and their PPI network is shown in **Fig. 3c**, where the GPT-GCG interaction exhibited the highest strength.

3.4 Construction and validation of biomarkers

To further screen the biomarkers, seven characteristic genes were screened by Lasso logistic regression (**Fig. 4a**). Next, 37 characteristic genes were obtained by Boruta (**Fig. 4b**). Subsequently, the hub gene was intersected with the genes that were screened via Lasso and Boruta to obtain four intersection genes, including GCG, SST, SLC30A10, and SLC22A5, which were recorded as biomarkers (**Fig. 4c**). The four biomarkers exhibited excellent diagnostic performance, with AUC values exceeding 0.9 in both the TCGA-CRC and GSE39582 datasets, indicating their robust power to distinguish CRC from control samples (**Fig 4d-e**).

3.5 Survival analysis and nomogram construction based on biomarkers

The TCGA-CRC samples were stratified into high and low expression groups based on the median value of biomarker expression. The K-M survival curve depicted a notable disparity in GCG expression between the two groups ($p = 0.023$) (**Fig. 5a**). Furthermore, we observed significant correlations between survival outcomes, tumor stage, and pathological TNM stage. The boxplot indicated that patients were more likely to have a high tumor stage and a high pathological TNM stage (**Additional file 3**). The nomogram illustrated the diagnostic performance of the biomarkers, and a calibration curve was used to assess its accuracy (**Fig. 5b**).

3.6 Functional analysis and immune analysis of biomarkers

An exploration of the biomarkers' biological functions via GSEA (**Fig. 6a**) identified significant pathway enrichments: GCG was linked to 105 pathways, SST to 91, SLC30A10 to 105, and SLC22A5 to 76. Notably, GCG was mainly linked to the drug metabolism cytochrome P450, neuroactive ligand receptor interaction, chemokine signaling pathway, and calcium signaling pathway. SST was concerned with chemokine signaling pathway, cell adhesion molecules, CAMs, neuroactive ligand receptor interaction, and hematopoietic cell lineage. There were significant associations between SLC30A10 and drug metabolism, cytochrome P450, chemokine signaling pathway as well as neuroactive ligand-receptor interaction. SLC22A5 was primarily associated with fatty acid metabolism, drug metabolism, cytochrome P450, and the metabolism of xenobiotics by cytochrome P450. Additionally, we compared the expression levels of 28 immune cell types between the CRC and normal groups **(Fig. 6b**). The results demonstrated that 22 immune cell types showed remarkable differences ($p < 0.05$) between these two groups. Furthermore, the Spearman correlation between biomarkers and differentially infiltrated immune cells was analyzed (**Fig. 6c**). Activated CD8 T cells showed a positive correlation with SST ($r = 0.415$, $p < 0.001$); in contrast, natural killer T cells were negatively correlated with SLC22A5 ($r = -0.370$, $p < 0.001$).

3.7 Prediction and construction of molecular regulatory network for biomarkers in CRC

A total of 489 DE-miRNAs were identified, with 199 up-regulated and 290 down-regulated (**Additional file 4**). In addition, 4,079 DE-lncRNAs were found, with 2,796 up-regulated and 1,283 down-regulated (**Additional file 5**). Subsequently, 489 DE-miRNAs identified 28 key miRNAs and 83 miRNAs from the miRnet database. Since the biomarkers were found to be down-regulated in CRC samples, we focused on identifying up-regulated intersecting 17 miRNAs that may potentially regulate their expression levels.

Through this approach, 93 key lncRNAs were identified by intersecting 4,079 DE-lncRNAs and 367 lncRNAs from the starbase database, which included 21 down-regulated lncRNAs. Finally, an lncRNA-miRNA-mRNA network was constructed (17 lncRNAs, 11 miRNAs, four mRNAs). LINC01140 regulated GCG and SLC30A10 through hsa-miR-146a-5p (**Fig. 7**).

3.8 Drug prediction and molecular docking analysis based on key genes

25 potential drugs targeting three biomarkers were predicted. Drug-gene network analysis showed that 16 drugs, including Naltrexone, Morphine, and Lornoxicam, targeted GCG. Seven drugs, such as Ganciclovir, Captopril, and Valinomycin, targeted SST. Two drugs targeted SLC22A5, including Imatinib and Carnitine (**Fig. 8a**). Molecular docking analysis revealed that Lornoxicam formed covalent bonds with residues ARG-290 and ARG-44 of the GCG protein, respectively (binding energy = -7.725 kcal / mol). Captopril established a covalent bond with residue GLU-57 of the SST protein (binding energy = -5.900 kcal/mol). Furthermore, Carnitine formed covalent bonds (binding energy = -6.261 kcal/mol) with residues SER-467, ARG-471, and TYR-447 of the SLC22A5 proteins (**Table 1, Fig. 8b**).

Targets	PDB ID	MolName	Docking score（kcal/mol）
GCG	7D6B	LORNOXICAM	-7.725
SST	7T10	CAPTOPRIL	-5.9
SLC22A5	AF-076082-F1	CARNITINE	-6.261

3.9 Expression validation of biomarkers

Biomarker expression was significantly higher in tumors versus controls, as shown in box plots consistent across datasets (**Fig. 9a-b**). This finding was confirmed by qRT-PCR in clinical tissues. In line with the analytical results from public databases, GCG, SST, SLC30A10, and SLC22A5 showed notably lower expression in clinical CRC samples relative to control samples (**Fig. 9c**).

4. Discussion

Lipids are a crucial component of the human physiological system, and the biological characteristics and functional equilibrium of biological membranes rely on their lipid composition. As second messengers and hormones, they also play a significant role in cellular signal transduction[29].In recent years, the association between lipid metabolism abnormalities and the progression of colorectal cancer (CRC) has attracted much attention: hyperlipidemia can reshape the lipid microenvironment of tumor cells, enhance the fluidity of cell membranes and vascular endothelial invasion ability, and drive CRC cells to metastasize to the liver via hematogenous metastasis.Much evidence suggests that hyperlipidemia assists CRC cells in entering the vascular system and migrating to the distant liver. A lifestyle with an HFD may enhance the stemness of CRC cells, thereby promoting their migratory capacity[30]. Hence, an in-depth investigation of lipid levels in CRC patients may be helpful for their

treatment. Additionally, screening and identifying molecular characteristics related to hyperlipidemia may help to explore the potential mechanism and further improve the outcomes for CRC patients.

The focus of our research was the expression of genes related to hyperlipidemia in CRC. Ultimately, we pinpointed four biomarkers (GCG, SST, SLC30A10, SLC22A5) which are strongly associated with CRC diagnosis and capable of acting as independent prognostic predictors. Glucagon (GCG), which is secreted by the alpha-cells of the Langerhans islets, serves as one of the primary hyperglycemic hormones in the body[31]. Alongside insulin, it helps maintain glucose homeostasis in the blood plasma[32]. As for the role of GCG in cancer, research findings have revealed that GCG can enhance the growth of human CRC cells cultivated in vitro[33,34] and potentially stimulate tumor angiogenesis by regulating the HIF-VEGF axis[35]. However, recent research suggests that glucagon can inhibit vascular endothelial cells' proliferation, migration, and tube formation. This property of glucagon makes it a potential target and marker for anti-angiogenic combination therapy in CRC[36]. The dysregulated GCG, with high prognostic value and connections to tumor progression and immunity, is a potential therapeutic target in CRC[37].

Somatostatin (SST), a somatogen inhibitor peptide, inhibits the growth and proliferation of tumor cells by binding to five different receptor subtypes, which play an essential anticancer role in various tumors[38,39]. Pre-operative serum methylated SST may serve as a novel prognostic marker in CRC, augmenting both the tumor staging system and serum CEA to enhance risk stratification[40]. SST might serve as aberrantly methylated-differentially expressed genes and pathways in the future[41]. Meanwhile, the PCR data generated in this study showed that SST had reduced expression in CRC samples. Therefore, it is speculated that the reduced expression of SST in CRC may be closely related to the occurrence and development of tumors. This reduction in expression may be related to the methylation status of SST gene, which then affects its function in tumor suppression.

Solute Carrier Family 30 Member 10 (SLC30A10) and Solute Carrier Family 22 Member 5 (SLC22A5) are essential members of the solute carrier transporter superfamily, actively involved in zinc (Zn) and manganese (Mn) transport, and play a significant role in apoptosis resistance. Zn is implicated in the progression of multiple cancer types[42], while Mn is a key metal for the activity of various cells[43]. Many studies have confirmed that SLC30A10 may be linked to neurodegenerative diseases[44]. Mutations in SLC30A10 can lead to Parkinson's disease[45], and reductions in SLC30A10 can also be seen in the brain anatomy of patients with Alzheimer's disease[46]. SLC30A10 is associated with methylation, epigenetic type, and molecular genesis of CRC[47]. Significant downregulation of SLC22A5 in CRC tissues versus normal adjacent tissues suggests a key tumor-suppressive role for this gene[48]. SLC30A10 and SLC22A5 are crucial for zinc and manganese transport and anti-apoptotic processes, and they have connections to a variety of diseases. The expression changes of SLC30A10 and SLC22A5 in colorectal cancer suggest their possible key role, which provides a basis for further study of their functions in cancer.

In this study, these four biomarkers had a strong ability to distinguish CRC patients into groups with different prognostic risks and were closely related to adverse prognostic factors such as tumor stage and pathological TNM stage. The nomogram based on the four biomarkers demonstrated high predictive accuracy and consistency for CRC prognosis, thus holding substantial clinical utility.

To further explore the biological functions of these four biomarkers, GSEA was performed. Among them, these biomarkers were closely related to “drug metabolism cytochrome P450” and “chemokine signaling pathway”. Some studies have shown that the “drug metabolism cytochrome P450” is upregulated in many types of cancers, such as hepatocellular carcinoma[49], gastric cancer[50], and lung cancer[51].Studies have demonstrated that cytochrome P4503A enzyme activity exists in both colorectal cancer tissues and healthy colonic epithelial cells. This enzyme enables cancer cells to inactivate anticancer drugs, potentially affecting tumor sensitivity to drug therapy [52]. Furthermore, primary colorectal cancers exhibit significantly higher expression levels of P450 enzymes such as CYP1B1 and CYP2S1 compared to normal colon tissue. Notably, elevated expression of CYP51 or CYP2S1 correlates with poor patient prognosis, with CYP51 serving as an independent prognostic marker[53]Thus,“drug metabolism cytochrome P450” might provide a valuable reference for the therapy of CRC. Additionally, studies have revealed that the "chemokine signaling pathway" is essential for foci-to-adenoma progression and adenoma-to-carcinoma progression[54]. Chemokines are chemotactic peptides that bind to G protein-coupled receptors, directing leukocyte migration and regulating cellular localization, which contributes to tumorigenesis[55]. Their production within the tumor microenvironment recruits host cells, promoting invasion and metastasis [56]. The significance of chemokine pathways in CRC is supported by bioinformatics studies[57], aligning with our results. This indicates that the biomarker-related pathways are critically involved in CRC progression, offering new perspectives for its management.

Using ssGSEA, we compared immune cell infiltration between CRC and normal groups. Consistent with the established roles of CD4+ and CD8+ T-cells in anti-tumor immunity[58], our analysis revealed a strong positive correlation between activated CD8+ T cells and SST, while both activated CD8+ T and effector memory CD4+ T cells were negatively correlated with SLC22A5. Furthermore, the abundance of several immune cells, including activated B cells, CD56dim NK cells, and macrophages, was significantly higher in CRC patients. This distinct immune cell landscape reflects the altered immune status in CRC, explaining the observed differences.

An lncRNA-miRNA-mRNA regulatory network was established to understand the regulatory mechanisms of biomarkers further. Here, we focused on the LincRNAs 1140 (LINC01140), which is overexpressed in gastric cancer and can be used as a biomarker to assess these patients' prognoses[59]. Moreover, upregulation of LINC01140 can protect c-Myc and PD-L1 mRNA from miRNA-mediated suppression, and promote lung cancer cells' growth, metastasis, and immune escape[60]. Recent evidence has found that hsa-miR-146a-5p is deregulated in various cancers, indicating that it may be a key tumor suppressor. For example, a study has demonstrated that hsa-miR-146a can significantly reduce prostate cancer cells' proliferation, invasion, and migration[61]. Other studies have suggested that miR-146a induces apoptosis

in prostate cancer by mediating the ROCK1/caspase3 pathway[62]. Considering that both LINC01140 and hsa-miR-146a-5p play critical regulatory roles in tumor progression, we speculated that LINC01140 might regulate the expression of GCG and SLC30A10 in CRC through hsa-miR-146a-5p, but more experimental verification is needed.

Finally, in order to further validate the association of biomarkers with clinical applications, we performed drug predictions. 16 therapeutic agents were predicted to target GCG, 7 drugs were predicted to target SST, and 2 drugs were predicted to target SLC22A5. Among them, molecular docking verified that these three biomarkers had good affinity with Lornoxicam, Captopril, and Carnitine. Lornoxicam is a non-steroidal anti-inflammatory drug (NSAID) used to treat joint and musculoskeletal diseases, such as osteoarthritis and rheumatoid arthritis[63]. Previous studies have shown that this drug contains various transition metals, such as Fe (II), Cr (III), and Cu(II), which have a strong inhibitory effect on the development of breast cancer cells and can be used as an alternative anti-tumor drug[64]. Recently, a study has shown that Lornoxicam is a new agent and small-molecule targeted drug candidate for treating CRC[65]. Captopril, an antihypertensive drug, has been shown to prevent obesity-related CRC, which seems to be linked to reduced chronic inflammation and oxidative stress[66,67]. Carnitine, a primary transporter for the acyl moiety of fatty acids to enter the mitochondrial matrix for oxidation[68], was reduced in CRC tissues compared to normal tissues in our project, which is inconsistent with previous reports[69]. Carnitine is also believed to significantly decrease cancer cells' proliferation and increase apoptosis[70], and a decrease in its content often indicates a decrease in mitochondrial lipid metabolites[71]. The biomarker-targeted drugs predicted in this study may be a new effective regimen for preventing and treating CRC.

Through analysis of hyperlipidemia-related gene expression in CRC, this study identified four key biomarkers (GCG, SST, SLC30A10, SLC22A5) and developed a prognostic model with robust predictive ability. There are also some limitations. Firstly, missing data and selection bias were inevitable since this was a retrospective project. Additionally, this study preliminarily explored the diagnostic value of hyperlipidema-related genes in CRC, and further experimental mechanism research is required, which are also the biomarkers we will focus on in our follow-up work. Finally, although this study confirmed that the characteristics of hyperlipidemia have significant prognostic value, more clinical applications are needed to clarify their function in CRC. We recommend that subsequent research involves multi-center clinical cohorts to verify the prognostic model's stability, alongside functional experiments to delve into the specific mechanisms of these four biomarkers in CRC.

5. Conclusion

In summary, we identified hyperlipidemia-related biomarkers, including GCG, SST, SLC30A10, and SLC22A5, and integrated these biomarkers to establish a risk nomogram and explore their potential value in diagnosing CRC. Our findings might provide new directions for studying the diagnose of CRC and contribute to the development of clinical prevention and therapy of CRC.

Abbreviations

Abbreviations	Full Names
CRC	colorectal cancer
HRGs	hyperlipidemia-related genes
DE-HRGs	differentially expressed HRGs
WGCNA	Weighted Gene Co-expression Network Analysis
PPI	Protein-Protein Interaction
ROC	receiver operating characteristic
qRT-PCR	quantitative reverse transcription polymerase chain reaction
EMT	epithelial-mesenchymal transition
HFD	high-fat diet
UCSC	University of California Santa Cruz
TCGA-COAD	The Cancer Genome Atlas-colon adenocarcinoma
TCGA-READ	The Cancer Genome Atlas-rectum adenocarcinoma
TCGA-CRC	The Cancer Genome Atlas-Colorectal cancer
DEGs	differentially expressed genes
FC	Fold Change
DGIDB	Drug-Gene Interaction database
GCG	Glucagon
SST	Somatostatin
SLC30A10	Solute Carrier Family 30 Member 10
SLC22A5	Solute Carrier Family 22 Member 5
Zn	zinc
Mn	manganese
GSEA	Gene set enrichment analysis
KEGG	Kyoto encyclopedia of genes and genomes
GO	Gene ontology

Declarations

Ethics approval and consent to participate

This study was performed in line with the principles of the Declaration of Helsinki. Approval was granted by the Science and Technology Ethics Committee of the Cancer Hospital Affiliated to Guangxi Medical University, and the approval number and date of approval are [KY2025042] and [on February 18, 2025]. Informed consent was obtained from all individual participants included in the study.

Consent for publication

Not applicable.

Availability of data and materials

The datasets analysed during the current study are available in The Cancer Genome Atlas (TCGA) database repository, [https://www.cancer.gov/ccg/research/genome-sequencing/tcga], and the Gene Expression Omnibus (GEO) database repository, [http://www.ncbi.nlm.nih.gov/geo/], and the GeneCards database repository, [http://www.genecards.org], and the DisGeNET database repository, [http://www.disgenet.org], and the DrugBANK database repository, [http://www.drugbank.ca].

Competing interests

The authors declare that they have no competing interests.

Funding

This study was supported by Joint Project on Regional High-Incidence Diseases Research of Guangxi Natural Science Foundation under Grant (2025GXNSFAA069077), Guangxi Traditional Chinese medicine suitable project technology development and promotion project (GZSY2025075).

Authors' contributions

Kunpeng Bu: Conceptualization, Data curation, Validation, Visualization, Writing–original draft, Writing–review & editing; Peigeng He: Data curation, Validation, Visualization, Writing–review & editing; Haiyan Huang:Data curation, Validation, Visualization, Writing–review & editing;Yue Wu: Validation, Writing–review & editing; Jinliang Kong: Conceptualization, Project administration, Supervision, Writing–review & editing. Tianwen Huang:Data curation, Validation, Visualization, Writing–review & editing.All authors read and approved the final manuscript.

Acknowledgements

We would like to express our sincere gratitude to all individuals and organizations who supported and assisted us throughout this research. Special thanks to the following authors: Peigeng He, Haiyan Huang,Yue Wu,Jinliang Kong,Tianwen Huang. In conclusion, we extend our thanks to everyone who has supported and assisted us along the way. Without your support, this research would not have been possible.

References

1. Sung H, Ferlay J, Siegel RL, et al. Global Cancer Statistics 2020: GLOBOCAN Estimates of Incidence and Mortality Worldwide for 36 Cancers in 185 Countries. CA Cancer J Clin, 2021, 71(3): 209-249.
2. Yang PM, Lin YT, Shun CT, et al. Zebularine inhibits tumorigenesis and stemness of colorectal cancer via p53-dependent endoplasmic reticulum stress. Sci Rep, 2013, 3: 3219.
3. Noonan SA, Morrissey ME, Martin P, et al. Tumour vasculature immaturity, oxidative damage and systemic inflammation stratify survival of colorectal cancer patients on bevacizumab treatment. Oncotarget, 2018, 9(12): 10536-10548.
4. Liu Y, Wang G, Yang Y, et al. Increased TEAD4 expression and nuclear localization in colorectal cancer promote epithelial-mesenchymal transition and metastasis in a YAP-independent manner. Oncogene, 2016, 35(21): 2789-800.
5. Long AG, Lundsmith ET, Hamilton KE. Inflammation and Colorectal Cancer. Curr Colorectal Cancer Rep, 2017, 13(4): 341-351.
6. Cappell MS. Pathophysiology, clinical presentation, and management of colon cancer. Gastroenterol Clin North Am. 2008 Mar;37(1):1-24.
7. Roshandel G, Ghasemi-Kebria F, Malekzadeh R. Colorectal Cancer: Epidemiology, Risk Factors, and Prevention. Cancers (Basel). 2024 Apr 17;16(8):1530.
8. Zheng X, Hur J, Nguyen LH, et al. Comprehensive Assessment of Diet Quality and Risk of Precursors of Early-Onset Colorectal Cancer. J Natl Cancer Inst, 2021, 113(5): 543-552.
9. Murphy N, Moreno V, Hughes DJ, et al. Lifestyle and dietary environmental factors in colorectal cancer susceptibility. Mol Aspects Med, 2019, 69: 2-9.
10. Morgan E, Arnold M, Gini A, et al. Global burden of colorectal cancer in 2020 and 2040: incidence and mortality estimates from GLOBOCAN. Gut, 2023, 72(2): 338-344.
11. De Almeida CV, De Camargo MR, Russo E, et al. Role of diet and gut microbiota on colorectal cancer immunomodulation. World J Gastroenterol, 2019, 25(2): 151-162.
12. Yang J, Wei H, Zhou Y, et al. High-Fat Diet Promotes Colorectal Tumorigenesis Through Modulating Gut Microbiota and Metabolites. Gastroenterology, 2022, 162(1): 135-149.e2.
13. Ren QW, Yu SY, Teng TK, et al. Statin associated lower cancer risk and related mortality in patients with heart failure. Eur Heart J, 2021, 42(32): 3049-3059.
14. Kahn CR, Wang G, Lee KY. Altered adipose tissue and adipocyte function in the pathogenesis of metabolic syndrome. J Clin Invest, 2019, 129(10): 3990-4000.
15. Nieman KM, Kenny HA, Penicka CV, et al. Adipocytes promote ovarian cancer metastasis and provide energy for rapid tumor growth. Nat Med, 2011, 17(11): 1498-503.
16. Hoy AJ, Balaban S, Saunders DN. Adipocyte-Tumor Cell Metabolic Crosstalk in Breast Cancer. Trends Mol Med, 2017, 23(5): 381-392.
17. Cozzo AJ, Fuller AM, Makowski L. Contribution of Adipose Tissue to Development of Cancer. Compr Physiol, 2017, 8(1): 237-282.

18. Love MI, Huber W, Anders S. Moderated estimation of fold change and dispersion for RNA-seq data with DESeq2. Genome Biol, 2014, 15(12): 550.
19. Langfelder P, Horvath S. WGCNA: an R package for weighted correlation network analysis. BMC Bioinformatics, 2008, 9: 559.
20. Gao CH, Yu G, Cai P. ggVennDiagram: An Intuitive, Easy-to-Use, and Highly Customizable R Package to Generate Venn Diagram. Front Genet, 2021, 12: 706907.
21. Wu T, Hu E, Xu S, et al. clusterProfiler 4.0: A universal enrichment tool for interpreting omics data. Innovation (Camb), 2021, 2(3): 100141.
22. Simon N, Friedman J, Hastie T, et al. Regularization Paths for Cox's Proportional Hazards Model via Coordinate Descent. J Stat Softw, 2011, 39(5): 1-13.
23. Li Z, Feng J, Zhong J, et al. Screening of the Key Genes and Signalling Pathways for Diabetic Nephropathy Using Bioinformatics Analysis. Front Endocrinol (Lausanne), 2022, 13: 864407.
24. Robin X, Turck N, Hainard A, et al. pROC: an open-source package for R and S+ to analyze and compare ROC curves. BMC Bioinformatics, 2011, 12: 77.
25. Liu TT, Li R, Huo C, et al. Identification of CDK2-Related Immune Forecast Model and ceRNA in Lung Adenocarcinoma, a Pan-Cancer Analysis. Front Cell Dev Biol, 2021, 9: 682002.
26. Hänzelmann S, Castelo R, Guinney J. GSVA: gene set variation analysis for microarray and RNA-seq data. BMC Bioinformatics, 2013, 14: 7.
27. Gustavsson EK, Zhang D, Reynolds RH, et al. ggtranscript: an R package for the visualization and interpretation of transcript isoforms using ggplot2. Bioinformatics, 2022, 38(15): 3844-3846.
28. Livak KJ, Schmittgen TD. Analysis of relative gene expression data using real-time quantitative PCR and the 2(-Delta Delta C(T)) Method. Methods. 2001 Dec;25(4):402-8.
29. Butler LM, Perone Y, Dehairs J, et al. Lipids and cancer: Emerging roles in pathogenesis, diagnosis and therapeutic intervention. Adv Drug Deliv Rev, 2020, 159: 245-293.
30. Karunanithi S, Levi L, Devecchio J, et al. RBP4-STRA6 Pathway Drives Cancer Stem Cell Maintenance and Mediates High-Fat Diet-Induced Colon Carcinogenesis. Stem Cell Reports, 2017, 9(2): 438-450.
31. Macdonald PE, Rorsman P. Metabolic Messengers: glucagon. Nat Metab, 2023, 5(2): 186-192.
32. Campbell JE, Newgard CB. Mechanisms controlling pancreatic islet cell function in insulin secretion. Nat Rev Mol Cell Biol, 2021, 22(2): 142-158.
33. Moyer MP, Aust JB, Dixon PS, et al. Glucagon enhances growth of cultured human colorectal cancer cells in vitro. Am J Surg, 1985, 150(6): 676-9.
34. Yagi T, Kubota E, Koyama H, et al. Glucagon promotes colon cancer cell growth via regulating AMPK and MAPK pathways. Oncotarget, 2018, 9(12): 10650-10664.
35. Wang Y, Zhu YD, Gui Q, et al. Glucagon-induced angiogenesis and tumor growth through the HIF-1-VEGF-dependent pathway in hyperglycemic nude mice. Genet Mol Res, 2014, 13(3): 7173-83.
36. Xu Y, Ni F, Sun D, et al. Glucagon Enhances Chemotherapy Efficacy By Inhibition of Tumor Vessels in Colorectal Cancer. Adv Sci (Weinh), 2024, 11(6): e2307271.

37. Du W, Miao Y, Zhang G, et al. The Regulatory Role of Neuropeptide Gene Glucagon in Colorectal Cancer: A Comprehensive Bioinformatic Analysis. Dis Markers, 2022, 2022: 4262600.
38. Reichlin S. Somatostatin. N Engl J Med, 1983, 309(24): 1495-501.
39. Kumar U. Somatostatin and Somatostatin Receptors in Tumour Biology. Int J Mol Sci, 2023, 25(1)： 436.
40. Liu Y, Chew MH, Tham CK, et al. Methylation of serum SST gene is an independent prognostic marker in colorectal cancer. Am J Cancer Res, 2016, 6(9): 2098-2108.
41. Liu J, Li H, Sun L, et al. Aberrantly methylated-differentially expressed genes and pathways in colorectal cancer. Cancer Cell Int, 2017, 17: 75.
42. Franklin RB, Costello LC. The important role of the apoptotic effects of zinc in the development of cancers. J Cell Biochem, 2009, 106(5): 750-7.
43. Huang L, Tepaamorndech S. The SLC30 family of zinc transporters - a review of current understanding of their biological and pathophysiological roles. Mol Aspects Med, 2013, 34(2-3): 548-60.
44. Go S, Kurita H, Yokoo K, et al. Protective function of SLC30A10 induced via PERK-ATF4 pathway against 1-methyl-4-phenylpyridinium. Biochem Biophys Res Commun, 2017, 490(4): 1307-1313.
45. Tuschl K, Clayton PT, Gospe SM, Jr., et al. Syndrome of hepatic cirrhosis, dystonia, polycythemia, and hypermanganesemia caused by mutations in SLC30A10, a manganese transporter in man. Am J Hum Genet, 2012, 90(3): 457-66.
46. Bosomworth HJ, Adlard PA, Ford D, et al. Altered expression of ZnT10 in Alzheimer's disease brain. PLoS One, 2013, 8(5): e65475.
47. Yagi K, Akagi K, Hayashi H, et al. Three DNA methylation epigenotypes in human colorectal cancer. Clin Cancer Res, 2010, 16(1): 21-33.
48. Zou D, Lou J, Ke J, et al. Integrative expression quantitative trait locus-based analysis of colorectal cancer identified a functional polymorphism regulating SLC22A5 expression. Eur J Cancer, 2018, 93: 1-9.
49. Tang L, Wei R, Chen R, et al. Establishment and validation of a cholesterol metabolism-related prognostic signature for hepatocellular carcinoma. Comput Struct Biotechnol J, 2022, 20: 4402-4414.
50. Wang DW, Su F, Yang LJ, et al. Bioinformatics Analysis and Identification of Potential Genes Associated with Pathogenesis and Prognosis of Gastric Cancer. Curr Med Sci, 2022, 42(2): 357-372.
51. Jin X, Liu X, Zhang Z, et al. Identification of key pathways and genes in lung carcinogenesis. Oncol Lett, 2018, 16(4): 4185-4192.
52. Martínez C, García-Martín E, Pizarro RM, García-Gamito FJ, Agúndez JA. Expression of paclitaxel-inactivating CYP3A activity in human colorectal cancer: implications for drug therapy. Br J Cancer. 2002 Sep 9;87(6):681-6.

53. Kumarakulasingham M, Rooney PH, Dundas SR, Telfer C, Melvin WT, Curran S, Murray GI. Cytochrome p450 profile of colorectal cancer: identification of markers of prognosis. Clin Cancer Res. 2005 May 15;11(10):3758-65.
54. Fayazfar S, Arefi Oskouie A, Safaei A, et al. Identification of key candidate genes and pathways associated with colorectal aberrant crypt foci-to-adenoma-to-carcinoma progression. Gastroenterol Hepatol Bed Bench, 2021, 14(Suppl1): S41-s50.
55. Itatani Y, Kawada K, Inamoto S, et al. The Role of Chemokines in Promoting Colorectal Cancer Invasion/Metastasis. Int J Mol Sci, 2016, 17(5).
56. Lazennec G, Richmond A. Chemokines and chemokine receptors: new insights into cancer-related inflammation. Trends Mol Med, 2010, 16(3): 133-44.
57. Yu C, Chen F, Jiang J, et al. Screening key genes and signaling pathways in colorectal cancer by integrated bioinformatics analysis. Mol Med Rep, 2019, 20(2): 1259-1269.
58. Yang Y, Feng M, Bai L, et al. The Effects of Autophagy-Related Genes and lncRNAs in Therapy and Prognosis of Colorectal Cancer. Front Oncol, 2021, 11: 582040.
59. Song P, Jiang B, Liu Z, et al. A three-lncRNA expression signature associated with the prognosis of gastric cancer patients. Cancer Med, 2017, 6(6): 1154-1164.
60. Xia R, Geng G, Yu X, et al. LINC01140 promotes the progression and tumor immune escape in lung cancer by sponging multiple microRNAs. J Immunother Cancer, 2021, 9(8).
61. Lin SL, Chiang A, Chang D, et al. Loss of mir-146a function in hormone-refractory prostate cancer. Rna, 2008, 14(3): 417-24.
62. Xu B, Huang Y, Niu X, et al. Hsa-miR-146a-5p modulates androgen-independent prostate cancer cells apoptosis by targeting ROCK1. Prostate, 2015, 75(16): 1896-903.
63. Ahmed MO, Al-Badr AA. Lornoxicam. Profiles Drug Subst Excip Relat Methodol, 2011, 36: 205-39.
64. Drakopoulou S, Kontis E, Pantiora E, et al. Effects of Lornoxicam on Anastomotic Healing: A Randomized, Blinded, Placebo-Control Experimental Study. Surg Res Pract, 2016, 2016: 4328089.
65. Unal U, Gov E. Drug Repurposing Analysis for Colorectal Cancer through Network Medicine Framework: Novel Candidate Drugs and Small Molecules. Cancer Invest, 2023, 41(8): 713-733.
66. Kubota M, Shimizu M, Sakai H, et al. Renin-angiotensin system inhibitors suppress azoxymethane-induced colonic preneoplastic lesions in C57BL/KsJ-db/db obese mice. Biochem Biophys Res Commun, 2011, 410(1): 108-13.
67. Shirakami Y, Shimizu M, Kubota M, et al. Chemoprevention of colorectal cancer by targeting obesity-related metabolic abnormalities. World J Gastroenterol, 2014, 20(27): 8939-46.
68. Console L, Scalise M, Mazza T, et al. Carnitine Traffic in Cells. Link With Cancer. Front Cell Dev Biol, 2020, 8: 583850.
69. Gold A, Choueiry F, Jin N, et al. The Application of Metabolomics in Recent Colorectal Cancer Studies: A State-of-the-Art Review. Cancers (Basel), 2022, 14(3).

70. Dionne S, Elimrani I, Roy MJ, et al. Studies on the chemopreventive effect of carnitine on tumorigenesis in vivo, using two experimental murine models of colon cancer. Nutr Cancer, 2012, 64(8): 1279-87.
71. Kang C, Zhang J, Xue M, et al. Metabolomics analyses of cancer tissue from patients with colorectal cancer. Mol Med Rep, 2023, 28(5).

Figures

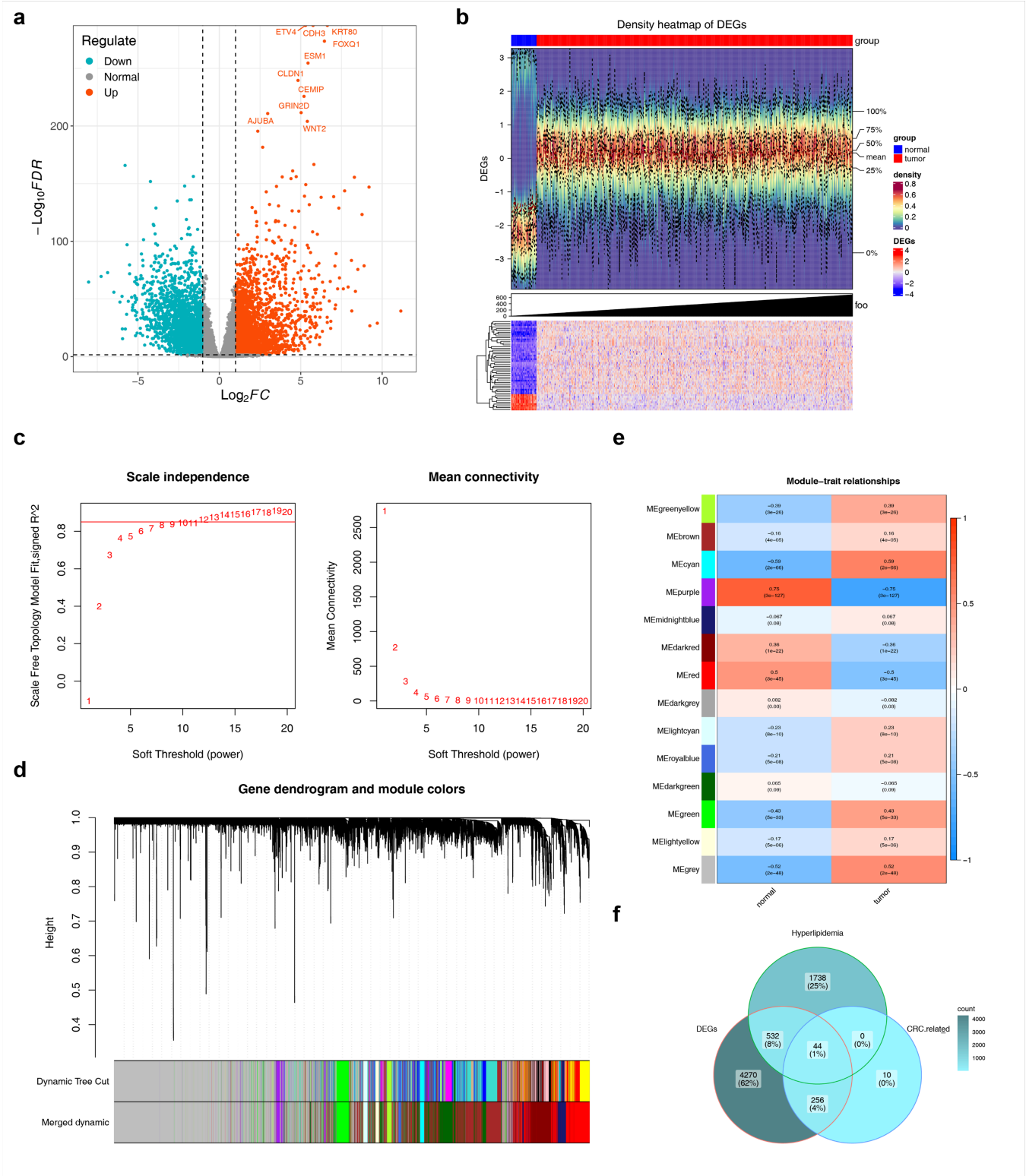


Figure 1

Identification of DE-HRGs in CRC. (a) Volcano plot of DEGs between CRC and normal samples. (b) Heatmap of the top 50 DEGs. (c) Analysis of scale-free fit index and mean connectivity for selecting the soft-thresholding power. (d) Cluster dendrogram of genes and identified co-expression modules. (e) Heatmap showing the correlation between module eigengenes and the CRC trait. (f) Venn diagram illustrating the intersection of DEGs, HRGs, and key module genes to identify DE-HRGs.

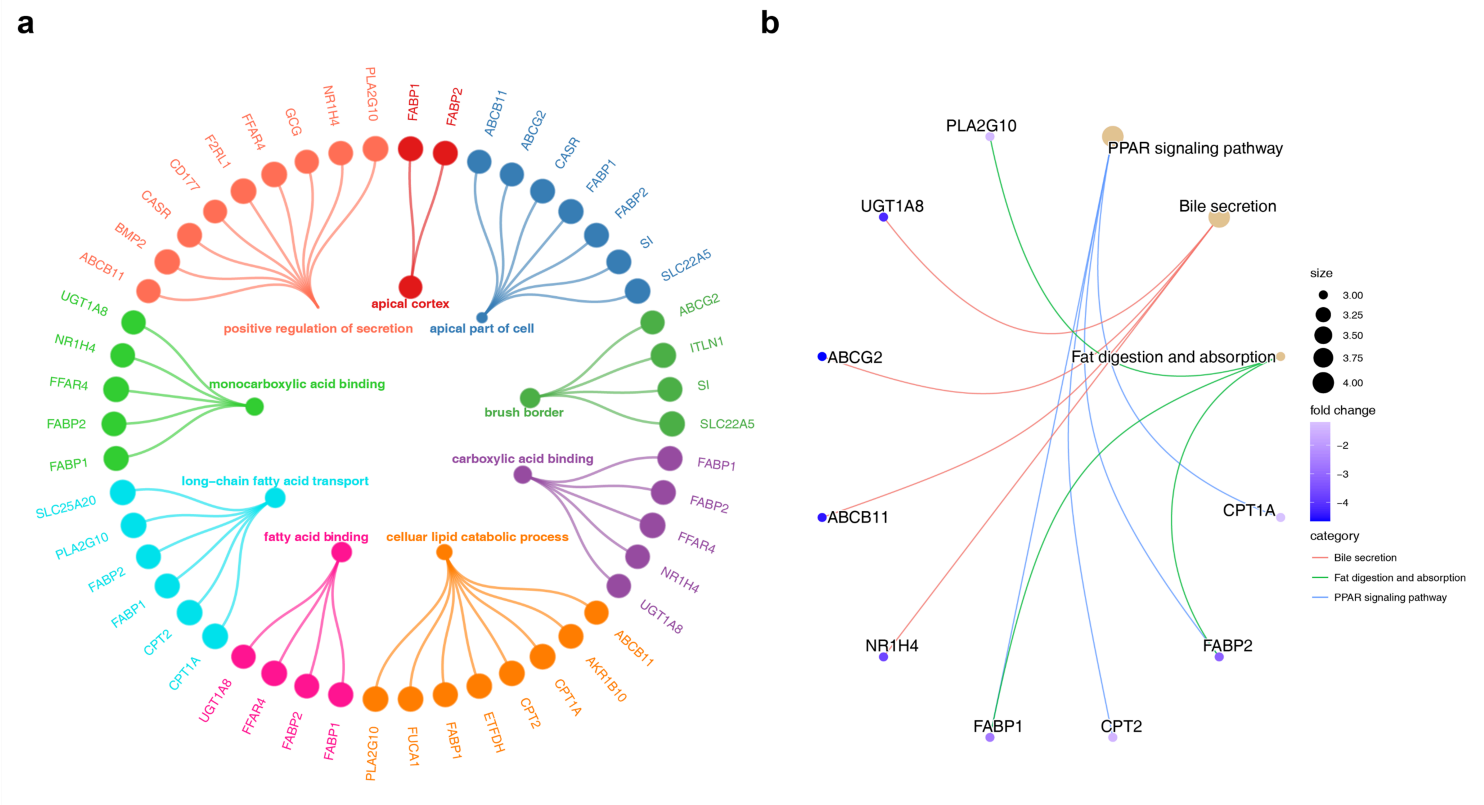


Figure 2

Functional Enrichment Analysis of 44 DE-HRGs. (a) Bar plot of the top three significantly enriched GO terms. (b) Chord plot of the top three significantly enriched KEGG pathways.

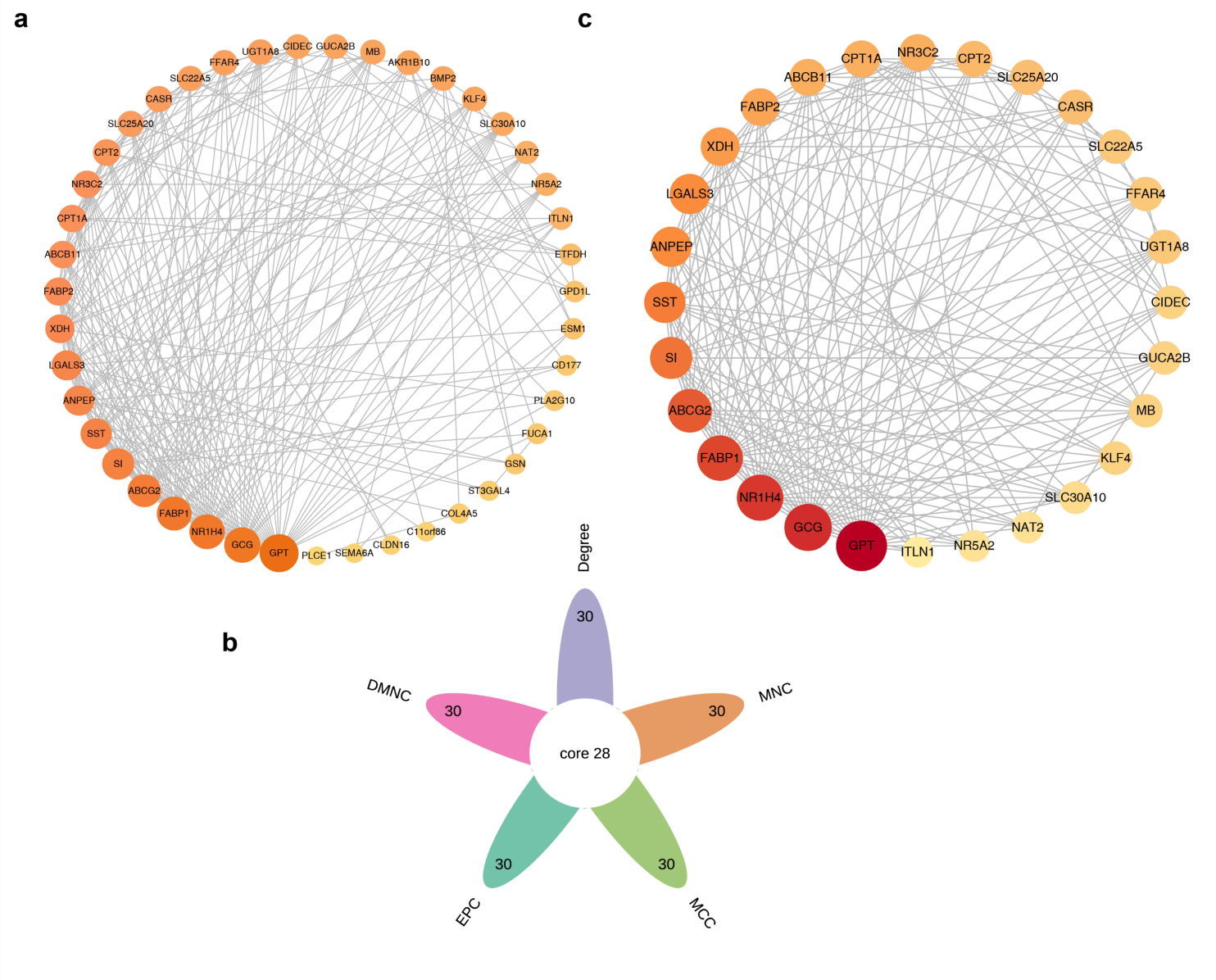


Figure 3

PPI Network and Hub Gene Identification. (a) PPI network of the 44 DE-HRGs. (b) Venn diagram showing the intersection of the top 30 genes identified by five algorithms (MCC, MNC, EPC, DMNC, Degree) from the PPI network. (c) PPI network of the 28 hub genes identified from the intersection.

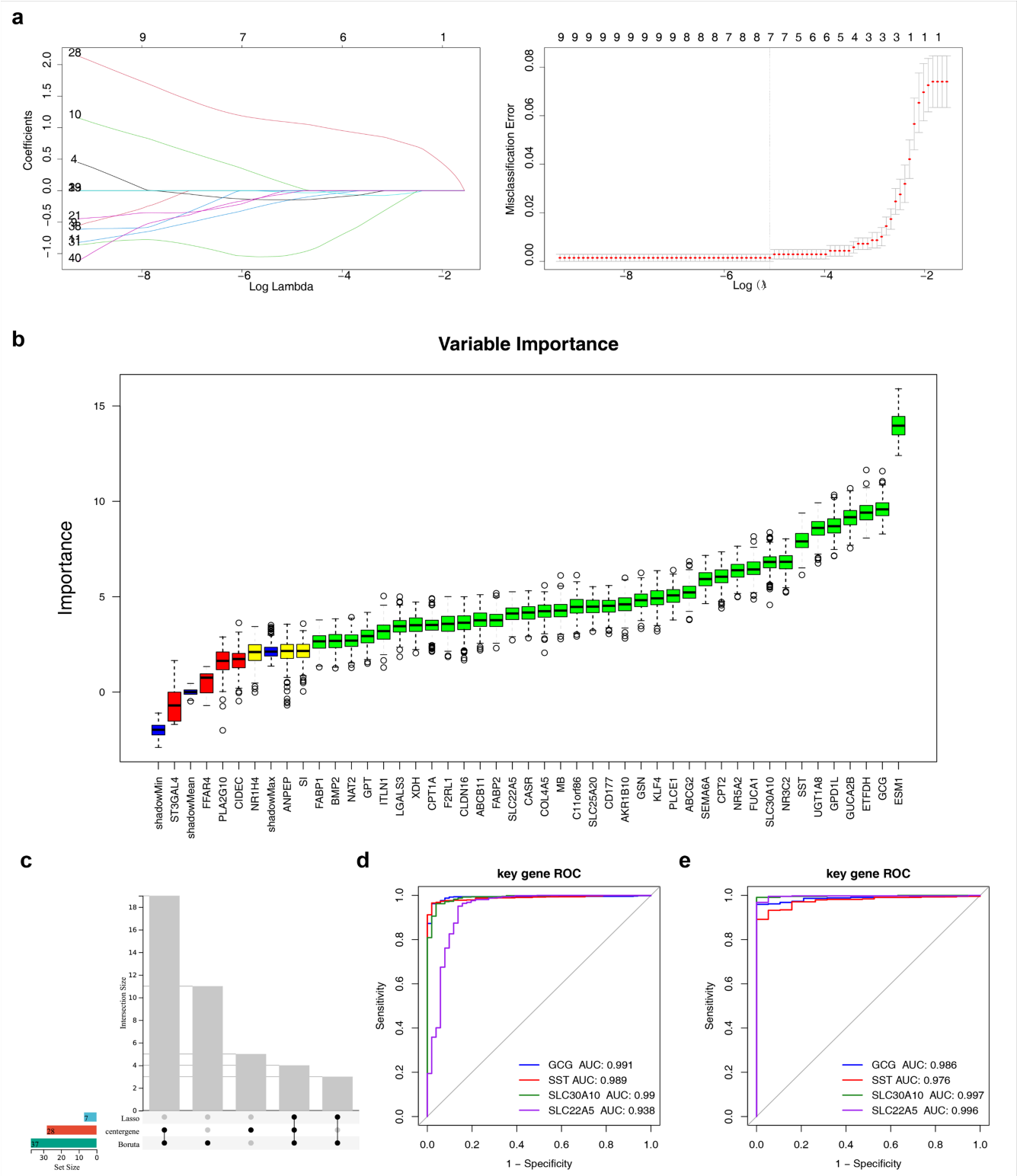


Figure 4

Screening and Validation of Diagnostic Biomarkers. (a-1) LASSO coefficient profiles of the DE-HRGs. (a-2) Selection of the optimal lambda (λ) parameter in the LASSO model. (b) Box plot of feature importance determined by the Boruta algorithm. (c) Venn diagram showing the intersection of hub genes and characteristic genes identified by LASSO and Boruta algorithms, defining the four biomarkers. (d) ROC

curves of the four biomarkers in the TCGA-CRC training set. (e) ROC curves of the four biomarkers in the GSE39582 validation set.

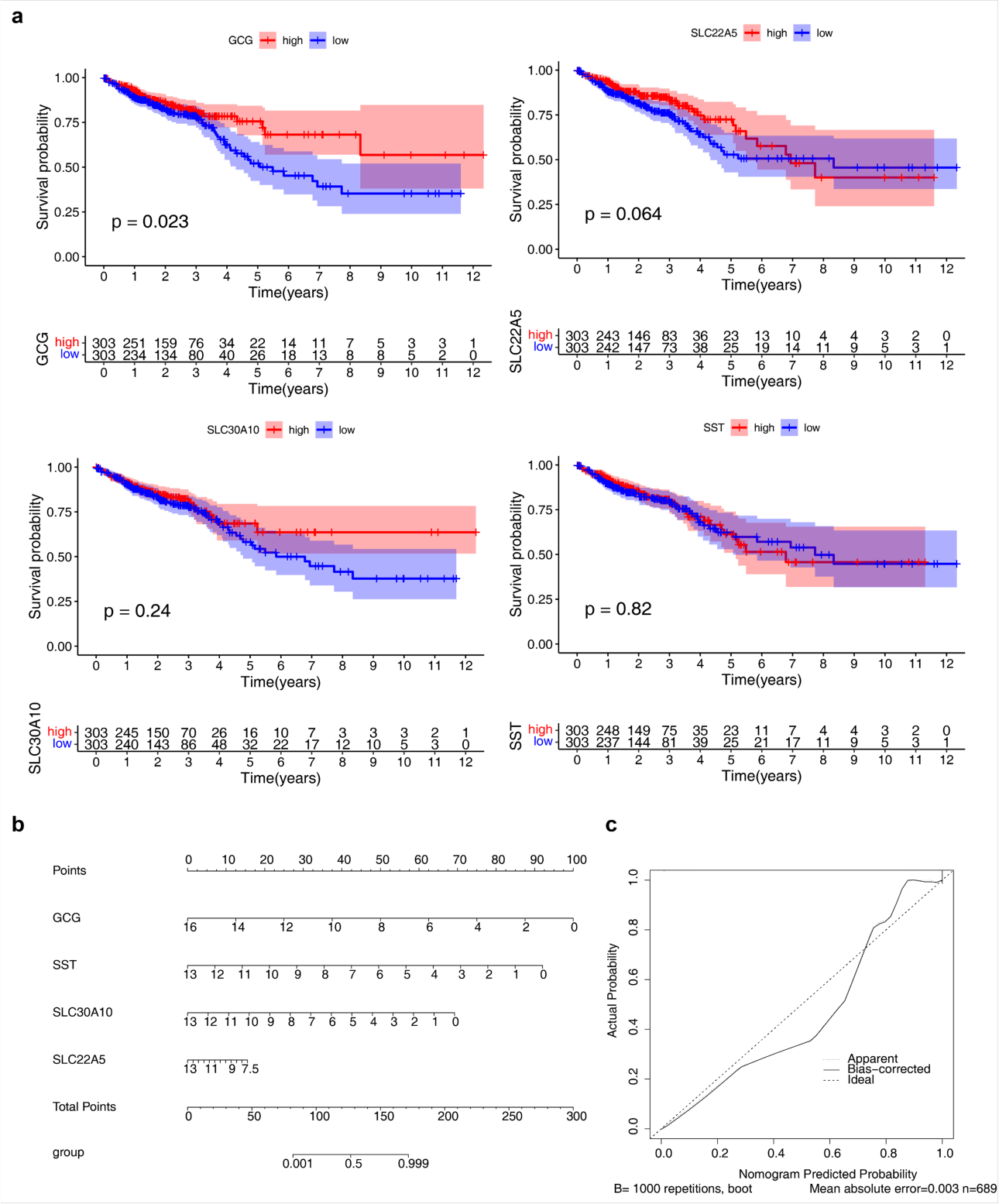


Figure 5

Survival Analysis and Nomogram Construction Based on Biomarkers. (a) Kaplan-Meier survival curves for CRC patients stratified by high and low expression of GCG. (b-1) Nomogram incorporating the four biomarkers for predicting CRC diagnosis probability. (b-2) Calibration curve of the nomogram.

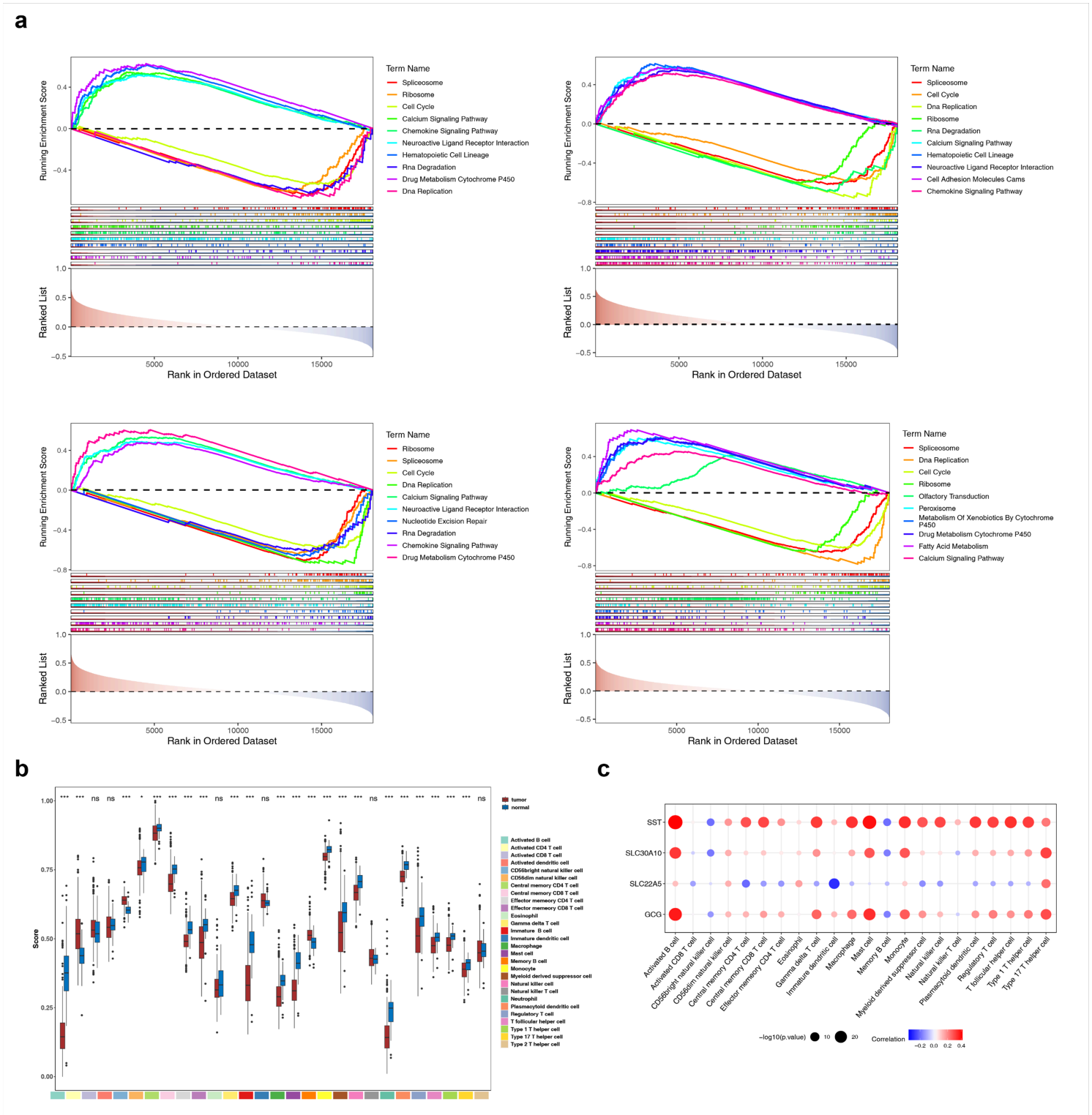


Figure 6

Functional Enrichment and Immune Infiltration Analysis of Biomarkers. (a) GSEA plots showing representative KEGG pathways enriched for each biomarker. (b) Box plots comparing the infiltration scores of 28 immune cell types between CRC and normal samples. (c) Heatmap showing the Spearman correlation between the four biomarkers and differentially infiltrated immune cells.

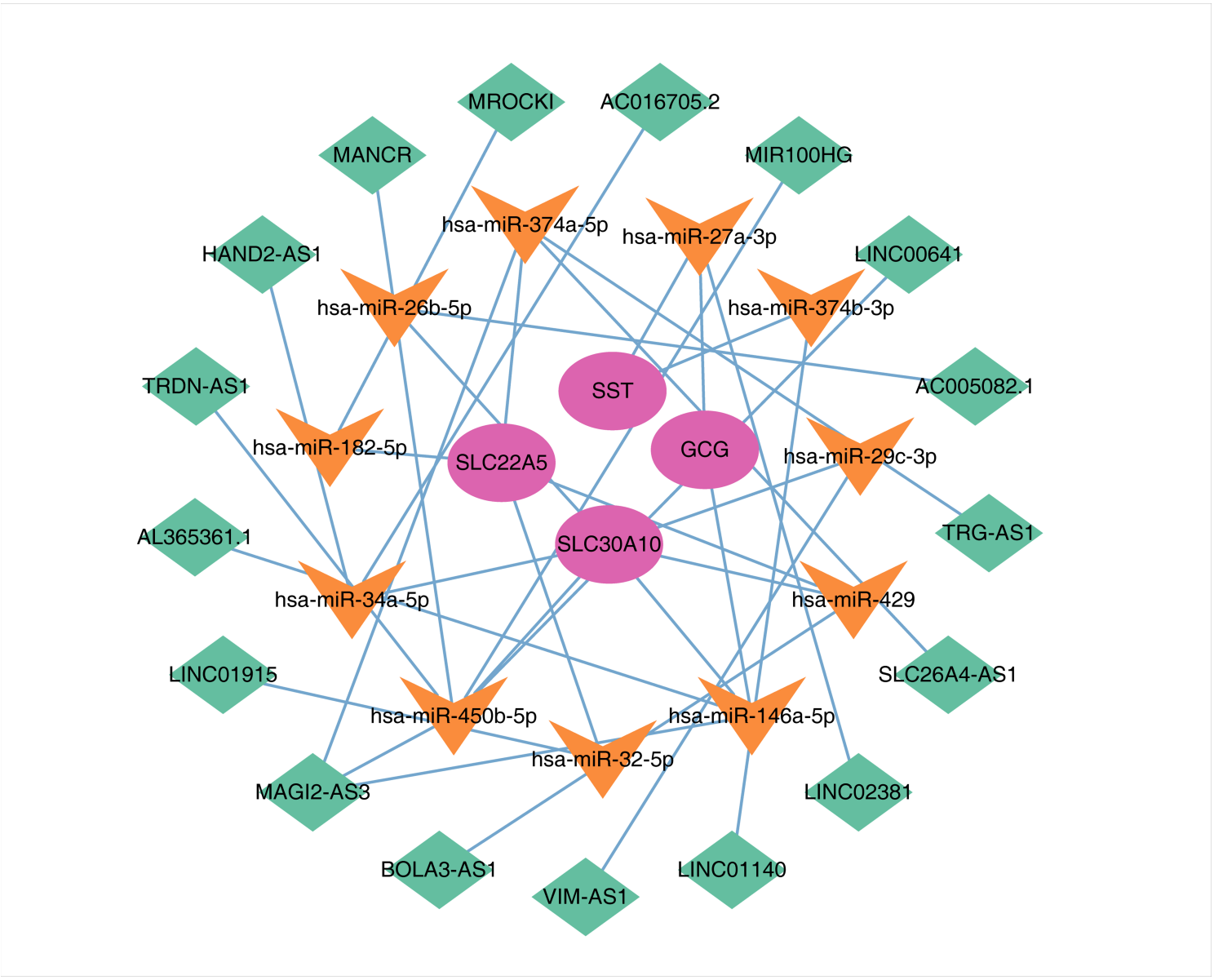


Figure 7

ceRNA Regulatory Network.

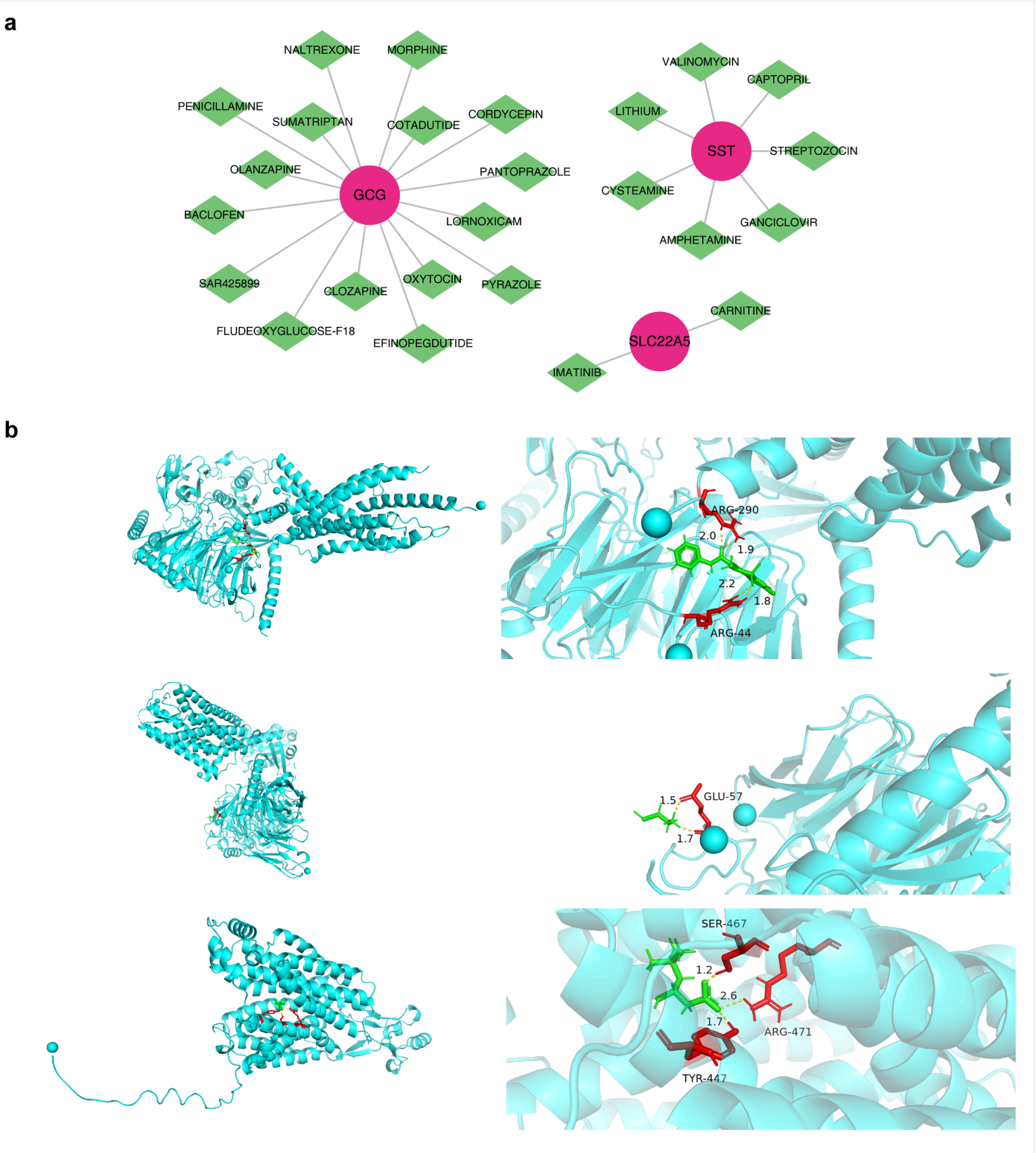


Figure 8

Drug Prediction and Molecular Docking for Biomarkers. (a) Network of predicted drug-gene interactions targeting the biomarkers. (b-1) Molecular docking model of GCG with Lornoxicam. (b-2) Molecular docking model of SST with Captopril. (b-3) Molecular docking model of SLC22A5 with Carnitine.

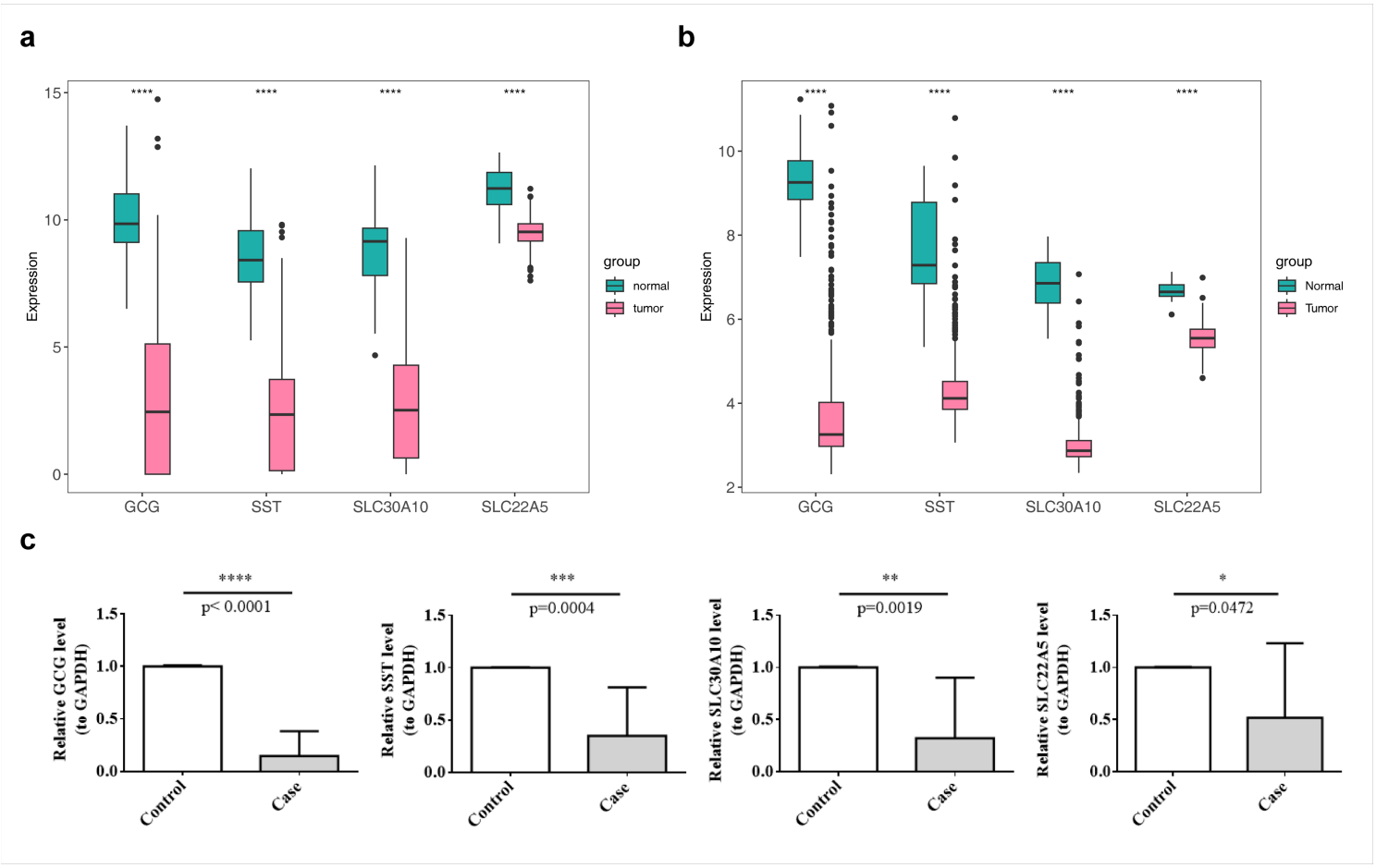


Figure 9

Expression Validation of the Four Biomarkers. (a) Box plots showing the expression levels of the four biomarkers in the TCGA-CRC training set. (b) Box plots showing the expression levels of the four biomarkers in the GSE39582 validation set. (c) qRT-PCR validation of the four biomarkers in clinical CRC and paired paracancerous tissues.

Supplementary Files

This is a list of supplementary files associated with this preprint. Click to download.

- Additionalfile1.docx
- Additionalfile2.tif
- Additionalfile3.tif
- Additionalfile4.tif
- Additionalfile5.tif